Princeton Plasma Physics Laboratory

PPPL-5310

Parametric Thermal and Flow Analysis of ITER Diagnostic Shield Module

A. Khodak, Y. Zhai, W. Wang, R. Feder, G. Loesser, D. Johnson

August 2016

Prepared for the U.S. Department of Energy under Contract DE-AC02-09CH11466.

Princeton Plasma Physics Laboratory
Report Disclaimers

Full Legal Disclaimer

Trademark Disclaimer

PPPL Report Availability

Princeton Plasma Physics Laboratory:

http://www.pppl.gov/techreports.cfm

Office of Scientific and Technical Information (OSTI):

http://www.osti.gov/scitech/

Related Links:

U.S. Department of Energy

U.S. Department of Energy Office of Science

U.S. Department of Energy Office of Fusion Energy Sciences

PARAMETRIC THERMAL AND FLOW ANALYSIS OF ITER DIAGNOSTIC SHIELD MODULE

A. Khodak, [a]* Y. Zhai, [a] W. Wang, [a] R. Feder, [a] G. Loesser, [a] D. Johnson [a]

[a]*PPPL, PO Box 451, Princeton University, NJ, 08543 USA*

akhodak@pppl.gov

As part of the diagnostic port plug assembly, ITER Diagnostic Shield Module (DSM) is designed to provide mechanical support and the plasma shielding while allowing access to plasma diagnostics. DSM 3 located in Equatorial Port Plug 9 and housing ITER Toroidal Interferometer and Polarimeter, (TIP) diagnostics was considered in current analysis.

Thermal and hydraulic analysis was performed using conjugated heat transfer approach, in which heat transfer was resolved in both solid and liquid parts, and simultaneously fluid dynamics analysis was performed only in the liquid part. This approach includes interface between solid and liquid part of the system. In such interface conservation of the heat flux is assumed together with the non-slip wall boundary conditions for the liquid. Since the flow in the cooling system is for the most part turbulent, non-slip wall boundary conditions take the form of wall functions.

ITER Diagnostic First Wall (DFW) and cooling tubing of the EPP09 DSM3 were also included in the analysis. This allowed direct modeling of the interface between DSM and DFW, and also direct assessment of the coolant flow distribution between the parts of DSM and DFW to ensure DSM design meets the DFW cooling requirements. Combined model of 2 DFWs and a DSM was imported in ANSYS Workbench. The model meshed contained 25 million elements, allowing accurate representation of the model details, as well as layers of elements on the fluid side of the fluid-solid

interface. Temperature dependent material properties were used in the analysis. Design of the DSM included voids filled with Boron Carbide pellets, allowing weight reduction while keeping shielding capability of the DSM. These voids were modeled as continuous solid with smeared material properties using analytical relation for thermal conductivity

Results of the analysis lead to design modifications improving heat transfer efficiency of the DSM. These modifications include rearrangement of the cooling channel sequence, and elimination of Boron Carbide beds in the front portion of the DSM to avoid local overheating. Analysis of the modified design showed that temperature does not exceed allowable values for DSM and DFW. Effect of design modifications on thermal performance as well as effect of Boron Carbide will be presented.

I. INTRODUCTION

During operation EPP09 DSM3 will include solid bodies as well as liquid coolant. Figure 1. shows solid and liquid parts of the heat transfer analysis, as well as solid-fluid interface surface which is colored with pressure distribution. Thermal and hydraulic analysis of the EPP09 DSM3 was performed using conjugated heat transfer approach, in which heat transfer was resolved in both solid and liquid parts, and simultaneously fluid dynamics analysis was performed only in the liquid part. This approach includes interface between solid and liquid part of the system. In such interface conservation of the heat flux is assumed together with the non-slip wall boundary conditions for the liquid. Since the flow in the cooling system is for the most part turbulent, non-slip wall boundary conditions take the form of wall functions.

Diagnostic First Wall (DFW) of the EPP09 DSM3 was also included in the analysis. This allowed direct modeling of the interface between DSM and DFW, and also direct assessment of the coolant flow distribution between the parts of DSM and DFW.

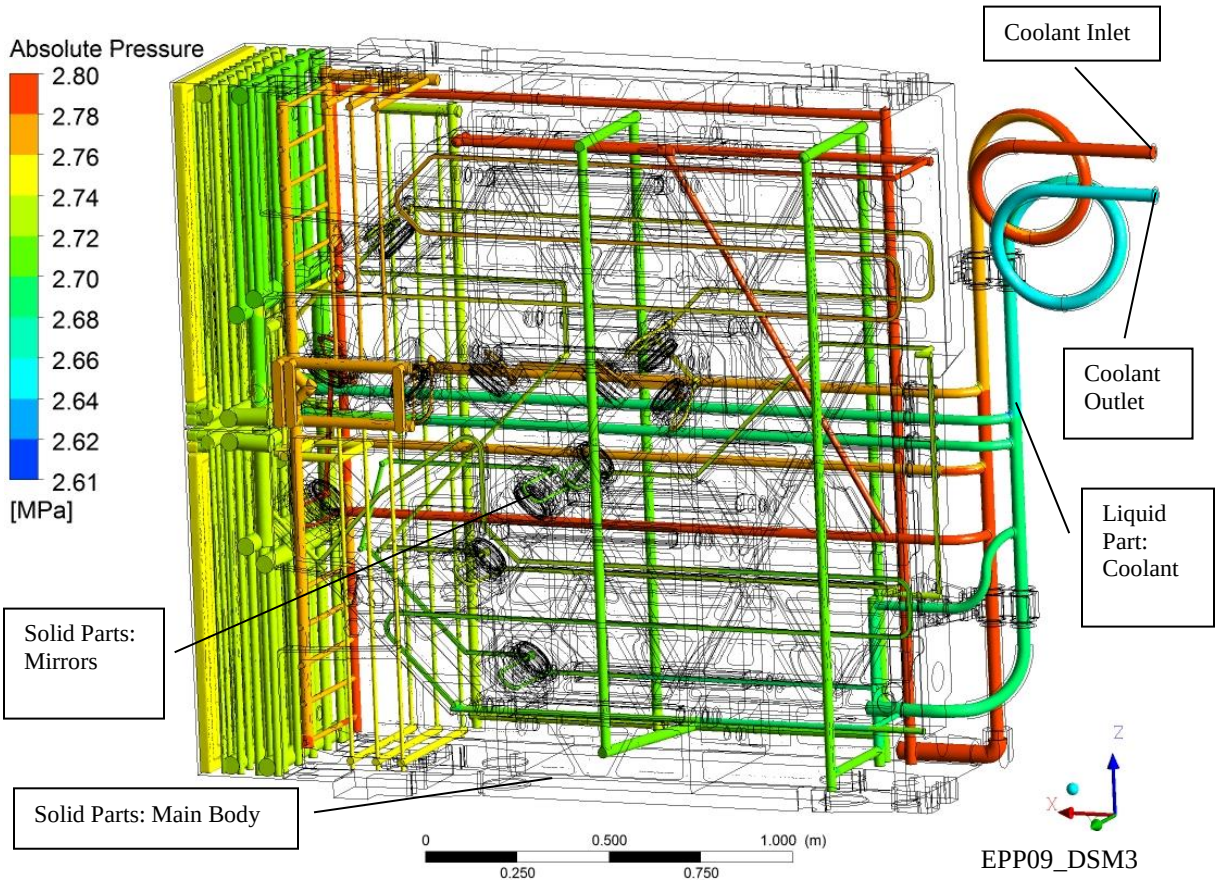

Fig. 1. Solid and liquid parts for conjugated heat transfer analysis. Pressure distribution is shown on the interface between solid and liquid parts.

Conjugated heat transfer analysis was performed using ANSYS CFX software. CFX software allows solution of heat transfer equations in solid and liquid part, and solution of the flow equations in the liquid part. Coolant flow in the DFW was assumed turbulent and was resolved using Reynolds averaged Navier-Stokes equations with Shear Stress Transport turbulence model. Detail description of the models used in the analysis is presented in [1].

II. HEAT TRANSFER ANALYSIS

II.A. Model Import and Simplification

Simplification of the EPP09 DSM3 model was performed in SolidWorks. Geometry was than imported directly from SolidWorks into ANSYS Workbench Design Modeller via STEP file. Geometrical simplifications included the following:

1. Hex nuts replaced with round cylinders
2. Bolted connections eliminated replaced with bonded connection with or without thermal resistance
3. Small geometrical features, at the dead end parts of the channels eliminated.
4. Volumes occupied by Boron Carbide filler are represented by voids in a solid structure.

Simplified model was imported into ANSYS Design Modeller where voids were filled creating volumes of Boron Carbide filler. Additionally coolant volume was created in a void defined by inner surfaces of the coolant channels between inlet and outlet.

II.B. Geometric Model Meshing for Fluid Flow and Heat transfer calculations

Meshing was performed using CFX method available within the framework of the ANSYS Workbench mesh generator. Combined mesh of more than 25 million elements was created for solid and liquid parts. Mesh included 3 near wall layers near boundaries in fluid region with inflation rate of 1.5 from initial value of 0.4 mm. Application of tetrahedral elements for meshing the internal regions, with triangular prism elements for boundary layers allowed automatic mesh generation. Unstructured tetrahedral automatic meshing algorithm was used. Boundary layers were imposed on all internal surfaces growing inside the fluid zone. Advanced sizing functions were used with automatic mesh inflation depending on wall proximity and curvature. Figure 2 shows representation of the mesh.

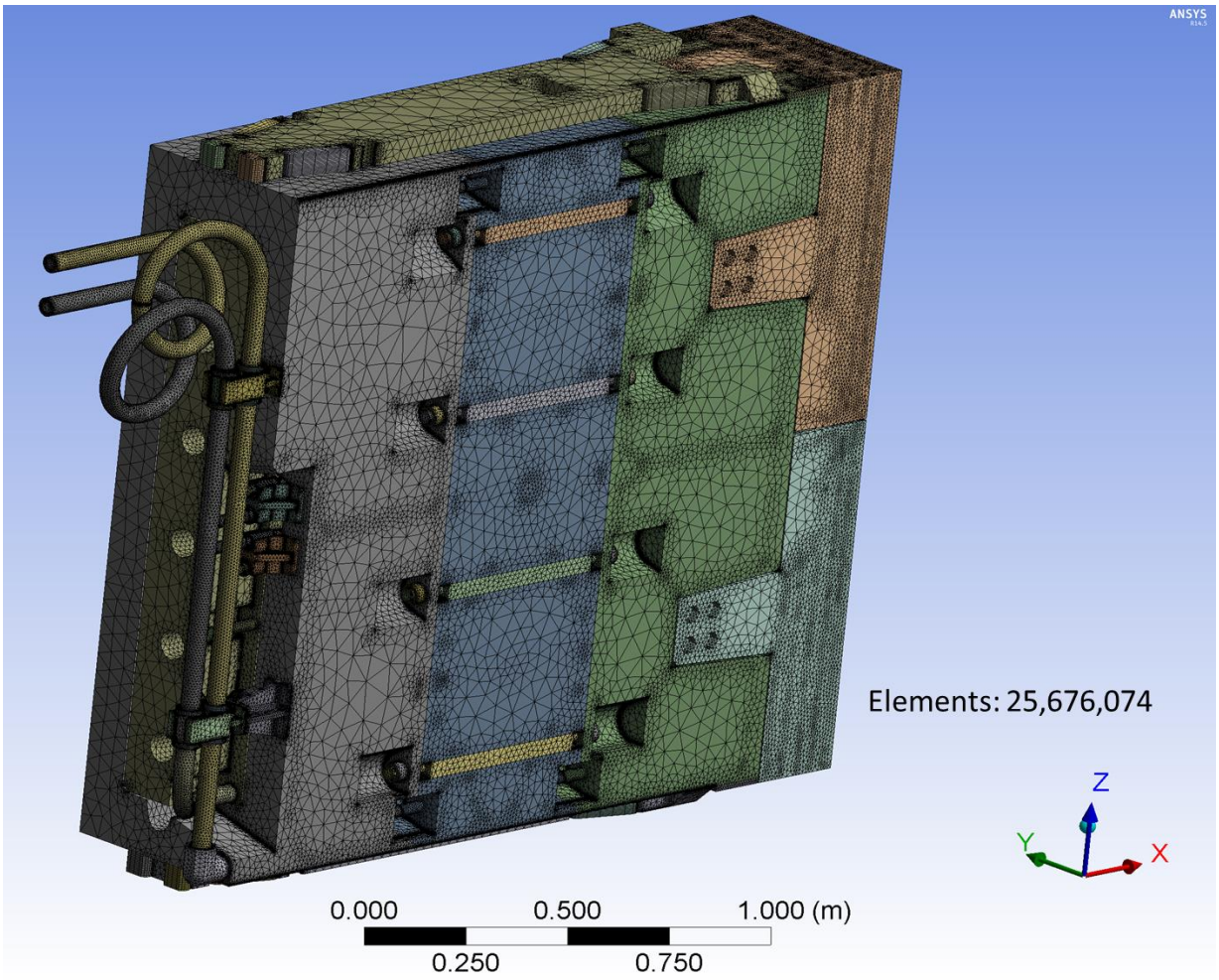

Fig. 2. EPP09 DSM3 mesh

Figures 3 and 4 show mesh cross-section in the body of the DSM and near the mirror. In both cases coolant channels were modeled with three layers of cells near solid walls. Mesh independence study of for this type of meshing was presented in [1].

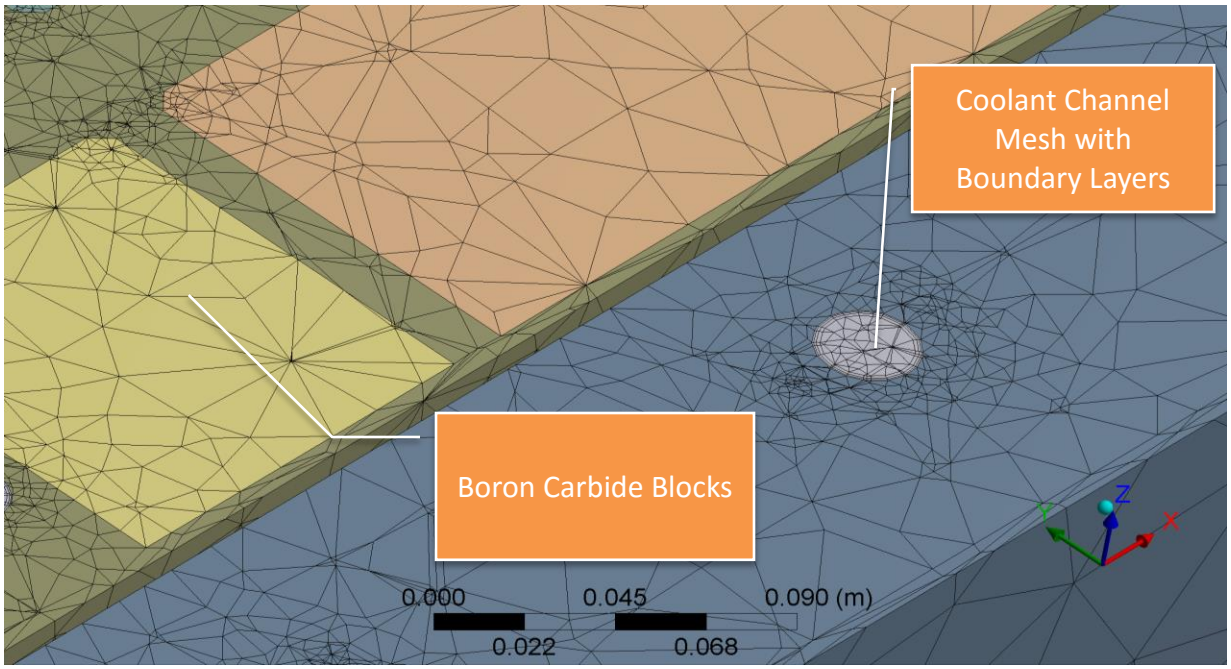

Fig. 3. EPP09 DSM3 mesh cross-section.

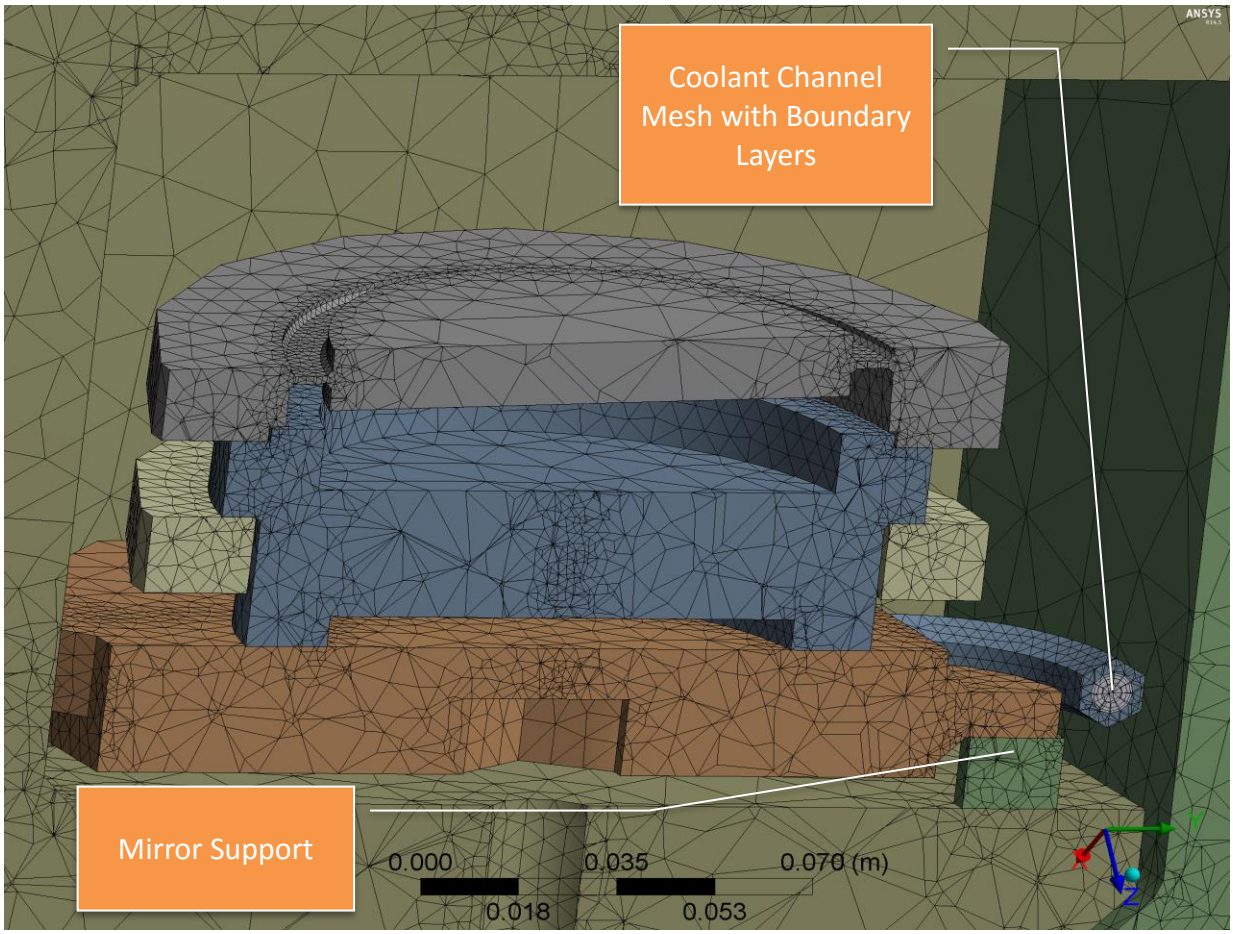

Fig. 4. EPP09 DSM3 mesh cross-section near mirror.

II.C. External Thermal Loads

Volumetric Heat Source distribution generated externally by Attila software was imported into CFX as described in [1]. Distribution of such variable for EPP09-DSM3 is presented on Figure 5 where it is compared to original Attila result.

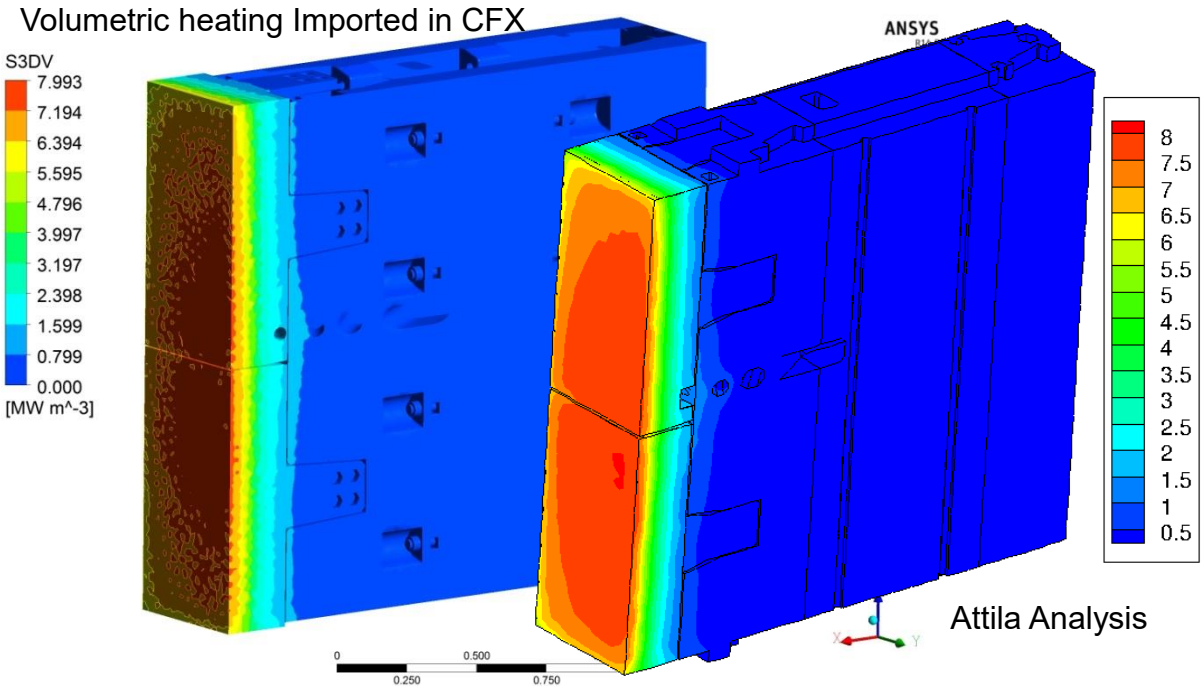

Fig. 5. Volumetric heating distribution.

Surface heating is presented on Figure 6. Constant heat flux of 350 kW/m2 was imposed on a front wall. Side wall heat flux was imposed using exponential formula

$$q_{side} = 0.5\, q_{front} e^{-x/G} \qquad (1)$$

where:

q_{side} - side heat flux

q_{front} - front heat flux of 350 kW/m2

G - gap width of 0.01 m

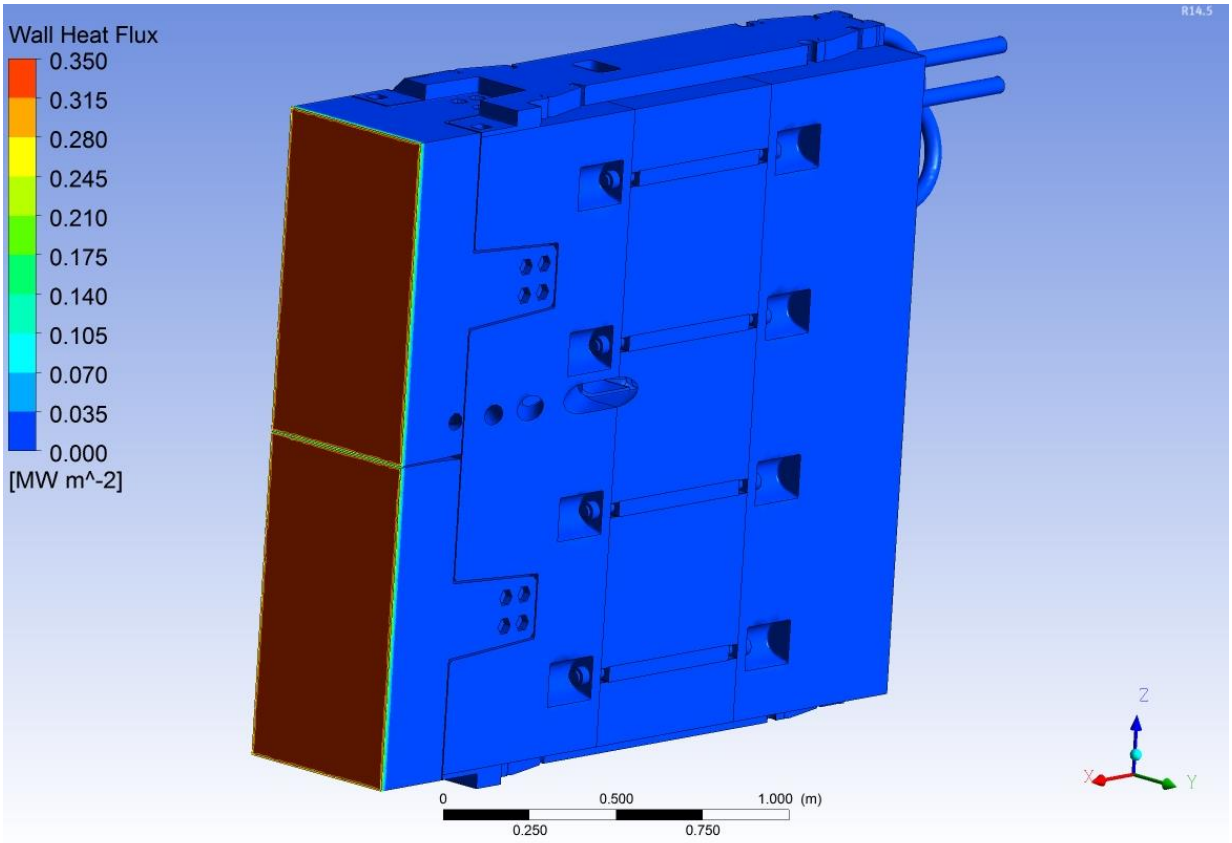

Fig. 6. Surface heat distribution.

II.D. Material Properties

The following materials were used in thermal analysis:

1. DSM, DFW, Bolts and Piping: Stainless Steel
2. Filler material: Packaged Boron Carbide (B4C)Pellets
3. Mirrors: Copper
4. Coolant: Water

Material properties used in thermal analysis are summarized in Table 1

Table 1. Material Properties used in the analysis

	B4C pure	Water	Copper	Stainless Steel
Specific Heat, J/g-°C	0.23	4.1817	0.385	0.434
Thermal Conductivity, W/m-K	30.0	variable	401.0	16.52
Density, g/cc	1.89	0.98	8.933	7.893

Coolant material is isotropic with the temperature dependent thermal conductivity and viscosity [1]. Properties of the Boron Carbide (B4C) Pellet Bed were considered smeared. Pellets of uniform shape and size are considered with the pellet diameter:

$$D_{pellet} = \left(\frac{3}{4\pi} V_{pellet}\right)^{1/3} \quad \text{where: } V_{pellet} = 0.25\text{E-}6 \text{ m}^3$$

B4C mass fraction in the bed is:

$$\delta_{B4C} = 0.77$$

So density of the bed is:

$$\rho_{B4Cbed} = \rho_{B4C} \cdot \delta_{B4C}$$

Pellets are packed in vacuum without any compression, so their contact surface is reduced to a point. Thus heat transfer is achieved by conduction through pellets and radiation exchange between the pellets. In this case formula proposed by Schotte [2] can be used. This formula assumes parallel conduction and radiation exchange in the pallet layer, and only radiation exchange between the pellet layers. In this case thermal conductivity o the B4C pellet bed is:

$$\lambda_{B4Cbed} = \frac{\delta_{B4C}}{\frac{1}{\lambda_{B4C}} + \frac{1}{\lambda_{rad}}} + (1 - \delta_{B4C})\lambda_{rad}$$

where:

λ_{B4C} = 30 [W/(mK)]- thermal conductivity of B4C

$\lambda_{rad} = 4\sigma\,\varepsilon T^3 D_{pellet}$

σ = 5.6704E-08 W/(m^{2}K^4) - Stefan-Boltzman constant

ε=1 - relative emissivity

T – local temperature [K]

Thermal conductivity o the B4C pellet bed is presented on Figure 7

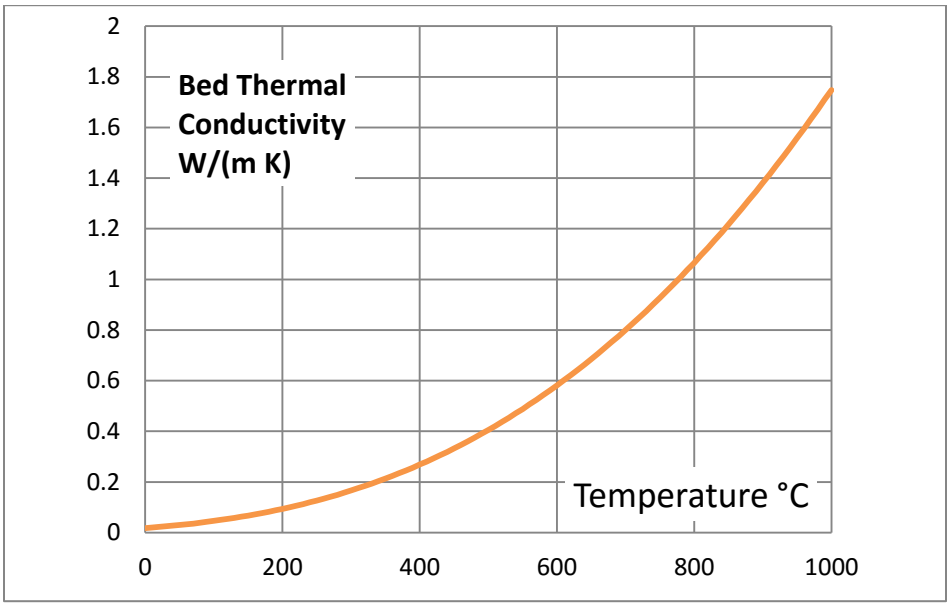

Fig. 7. Thermal conductivity o the B4C pellet bed

III. ANALYSIS RESULTS AND MODIFICATIONS

III.A. DSM Temperature Distributions

Design of the ITER TIP DSM includes optical cassette with multiple mirrors allowing easier mirror alignment. Temperature distribution on the DSM is presented on Figure 8. Results show that water

cooling system presented on Figure 1 can efficiently cool down DSM unit. Main source of heat of the DSM is volumetric heating, which declines at exponential rate from front to back. Maximum temperature in DSM is below 240°C.

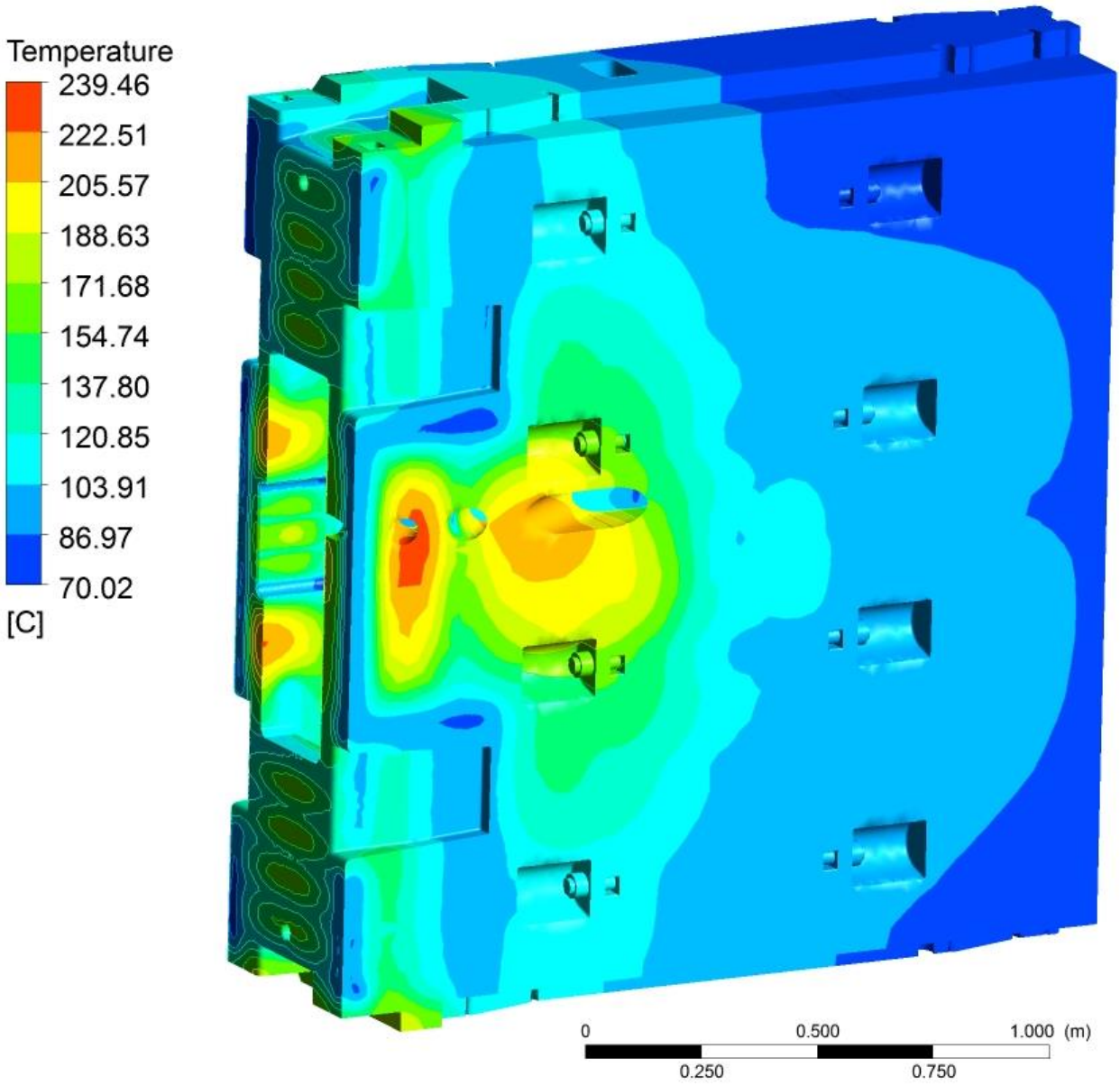

Fig. 8. DSM temperature distribution.

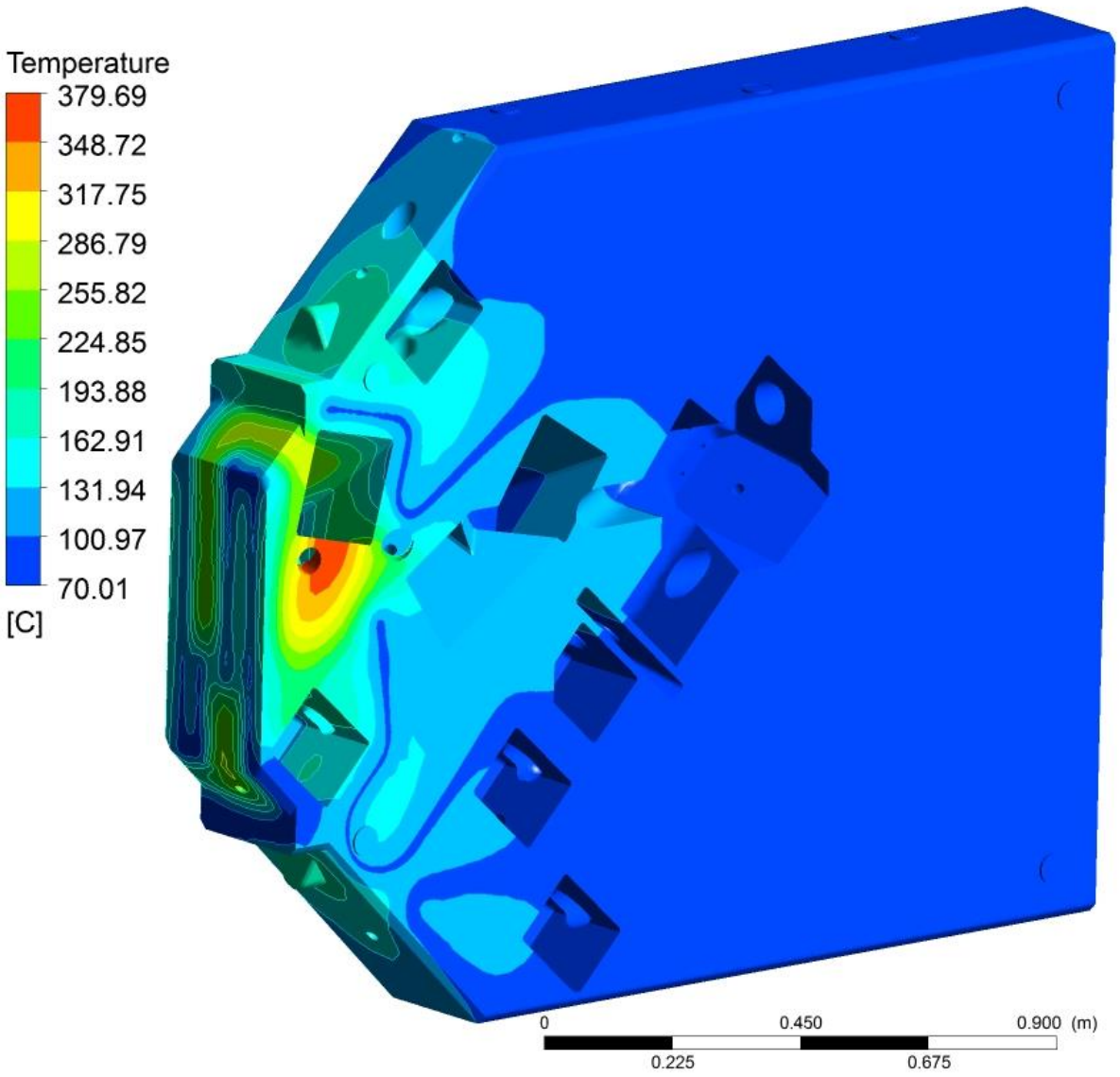

Fig. 9. Cartridge temperature distribution.

Figure 9 shows cartridge temperature distribution. Maximum temperature is below 400°C. The hot spot is localized in the front of the cartridge. As with the DSM cooling system for the cartridge cooling system presented on Figure 10 consists of a combination gun drilled, and milled channels. The local hot spot on the cartridge can be eliminated by rerouting the mill channel.

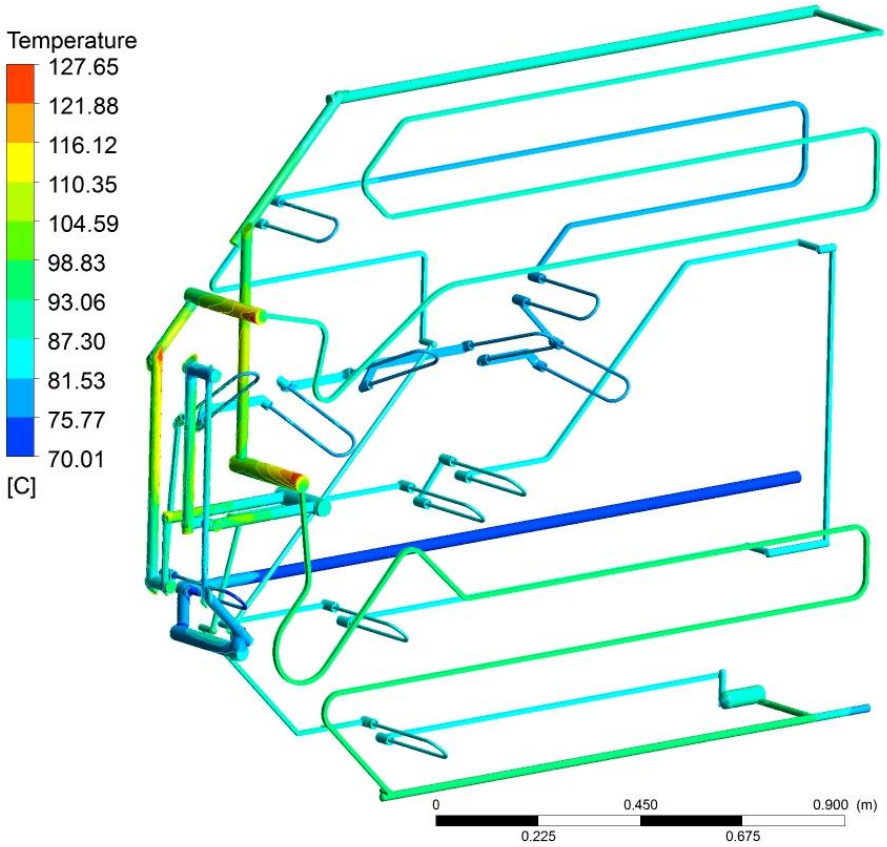

Fig. 10. Cartridge cooling system temperature distribution.

Keeping temperature variations on the mirrors to a minimum is very important for successful operation of the TIP front optics. ITER TIP cartridge cooling system includes horseshoe channels cooling mirror bases. Figure 11 shows temperature distribution on mirrors. Results show 1°C on the mirror surface of the hottest mirror.

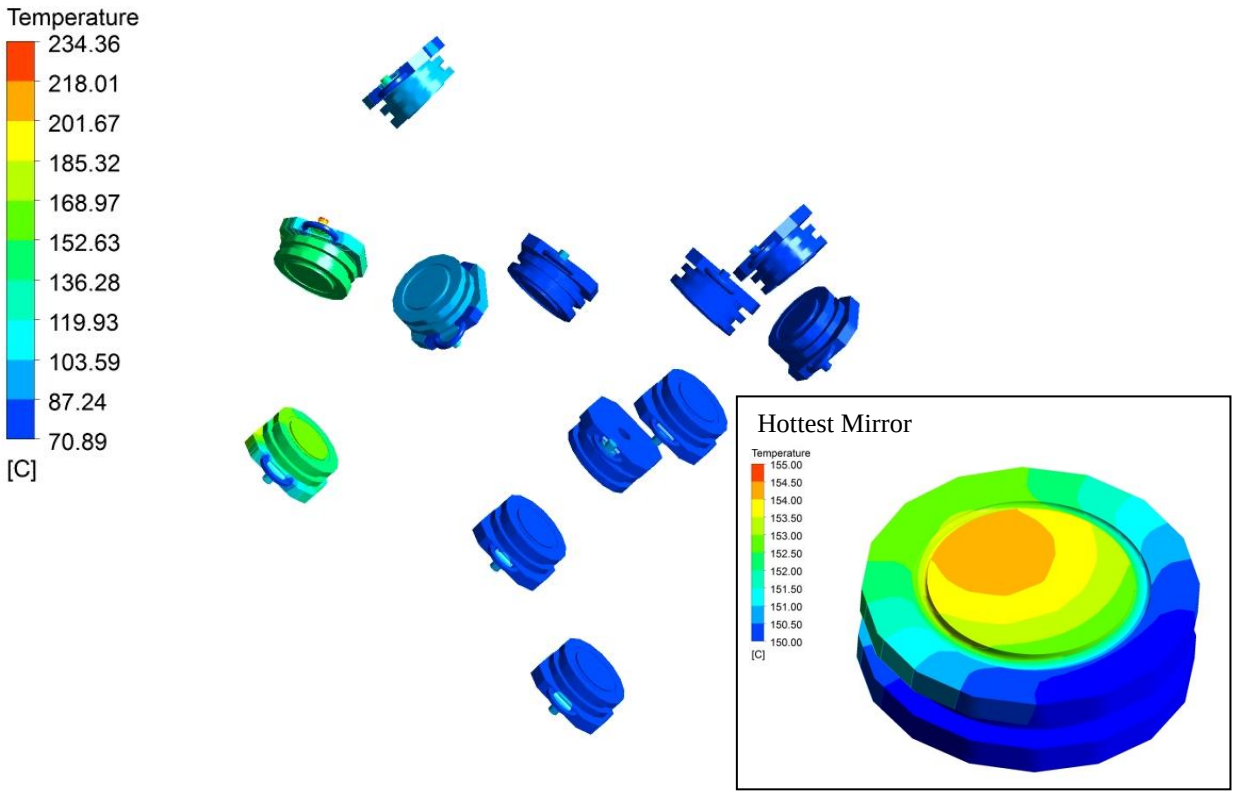

Fig. 11. Temperature distribution on mirrors.

III.B. Design Modifications

During design process supply tubing was rearranged from sequential arrangement of DSM and cartridge to parallel as shown on Figure 12. Parallel arrangement allowed efficient cooling of the DSM and cartridge by delivering cold water to the front of both units.

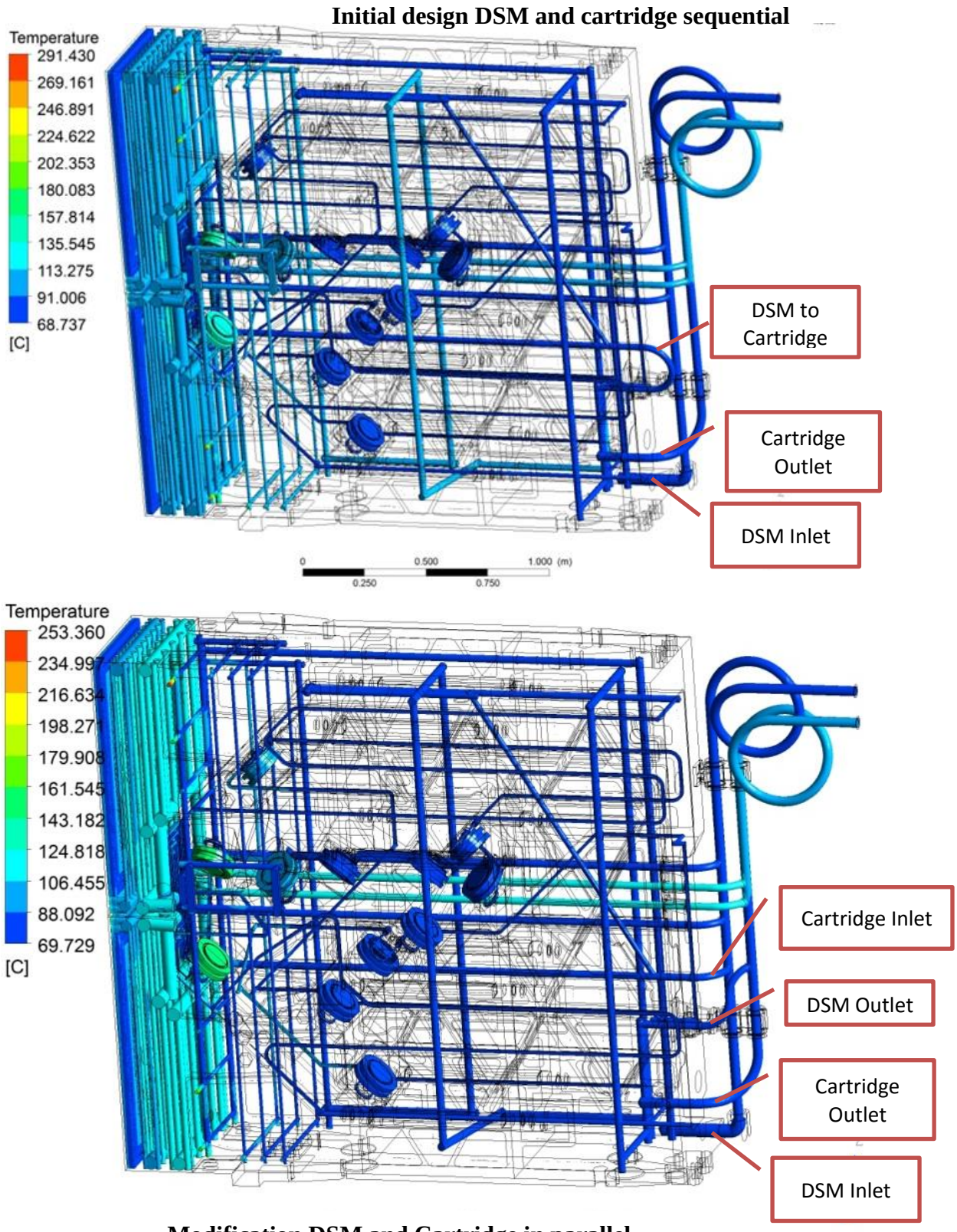

Fig. 12. UPP18L DFW initial design.

To reduce overall mass of the DSM, voids were created in the steel portions of DSM and cartridge. These voids are filled with Boron Carbide (B4C) granular bed. This allows mass reduction, while maintaining the same absorption of neutrons. Granular bed has very low thermal conductivity, thus B4C regions in the front portion of the DSM and cartridge were eliminated during the design process, because of excessive temperature. Final arrangement of the B4C filler is presented on Figure 13. Table 2 shows that mass of the voids filled with B4C granular bed is 652.1 kg, whereas if the same void is filled with steel the mass would be 3584.9 kg. Thus introduction of B4C filler allow reducing mass of DSM and cartridge by 2932.8 kg.

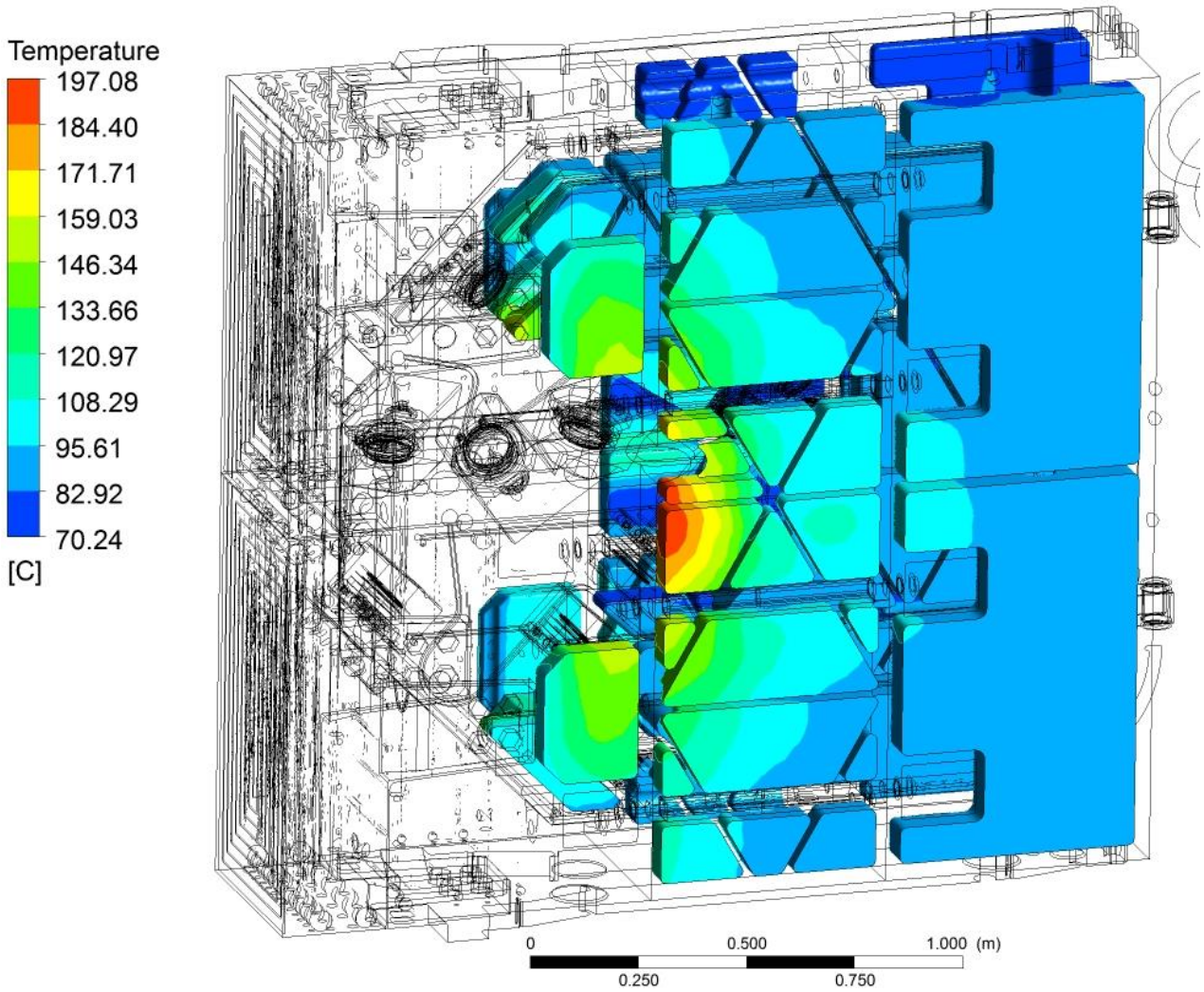

Fig. 13. UPP18L DFW initial design.

Table2. Analysis Results Summary

	Mass		Coolant Flow		Max T	Heat Load	
	[kg]	% total	[k/s]	% total	[C]	[kW]	% total
DSM	5839.0	49.6%	1.024	14.6%	239.5	60.74	5.8%
Cartridge	3054.8	26.0%	0.384	5.5%	379.7	30.74	2.9%
Voids filled with B4C	652.1	5.5%			290.5	0.77	0.1%
Mirrors	144.9	1.2%			154.4	1.86	0.2%
Rails	438.2	3.7%			184.0	1.99	0.2%
DFW	1536.0	13.1%	5.593	79.9%	541.9	959.12	90.9%
Tubing	97.8	0.8%			138.5	0.28	0.0%
Total	**11762.8**	**100.0%**	**7.000**	**100.0%**		**1055.50**	**100.0%**
Coolant	93.3	0.8%			131.6	249.90	23.7%
Voids if filled with steel	3584.9	23.4%					

III.C. Diagnostics First Wall Temperature Distributions

Initial model for DFW and supply tubing were also included in overall analysis. This way performance and the flow balance of the whole cooling system can be analyzed. Temperature distribution on DFW and supply tubing is presented on Figure 14. Excessive high temperature zones occur on the edges of the front wall of the DFW, and can be eliminated during detailed modeling of DFW, which is out of scope of this study. Overall balance of the coolant flow distribution and heat loads in all parts are presented on Table 2.

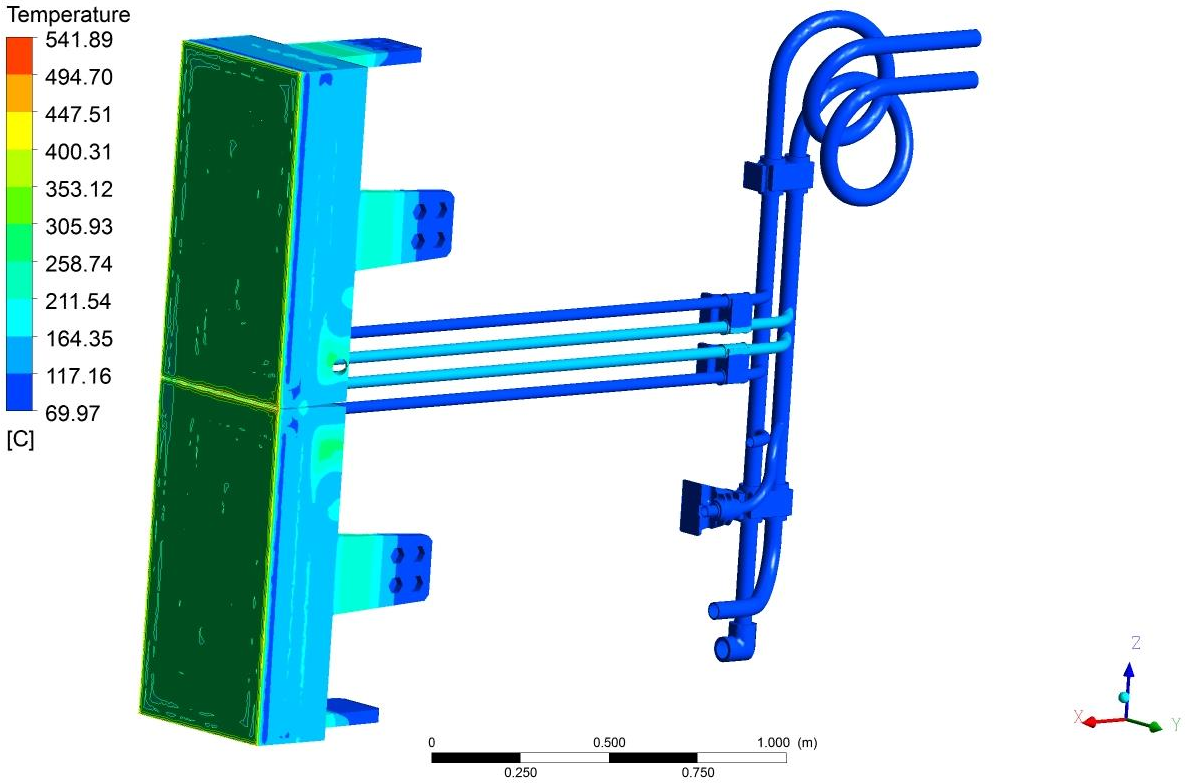

Fig. 14. Temperature distribution on Diagnostics First Wall and supply tubing.

IV. CONCLUSIONS

Numerical simulations of the coolant flow and heat transfer in ITER diagnostic shield module together with diagnostics first walls were performed using ANSYS CFX and included: 3D coolant flow analysis; external volumetric and surface heating effect.

Based on the analysis, modifications of the design were introduced to reduce temperature non-uniformity on the front optics mirrors.

Introduction of B4C volumes in the DSM allows significant weight reduction, without significant increase in temperature levels, when B4C are avoided in the front portion of the DSM.

ACKNOWLEDGMENTS

The views and opinions expressed herein do not necessarily reflect those of the ITER Organization.

REFERENCES

1. A. E. KHODAK et al., “Numerical Analysis of Coolant Flow and Heat Transfer in ITER Diagnostic First Wall,” *Fusion Sci. Technol.*, **68**, *10*, 521-525 (2015).
2. W. SCHOTTE, " Thermal Conductivity of Packed Beds," *A.I.Ch.E. Journal*, **6**, *1*, 63-67 (1960).

PPPL PRINCETON PLASMA PHYSICS LABORATORY

Princeton Plasma Physics Laboratory
Office of Reports and Publications

Managed by
Princeton University

under contract with the
U.S. Department of Energy
(DE-AC02-09CH11466)

P.O. Box 451, Princeton, NJ 08543
Phone: 609-243-2245
Fax: 609-243-2751

E-mail: publications@pppl.gov

Website: http://www.pppl.gov